ARR No. 5A08

NATIONAL ADVISORY COMMITTEE FOR AERONAUTICS

WARTIME REPORT

ORIGINALLY ISSUED

April 1945 as
Advance Restricted Report 5A08

AN INVESTIGATION OF AIRCRAFT HEATERS

XX - MEASURED AND PREDICTED PERFORMANCE OF A FINNED-TYPE CAST-ALUMINUM CROSSFLOW EXHAUST GAS AND AIR HEAT EXCHANGER

By L. M. K. Boelter, A. G. Guibert, J. M. Rademacher,
F. E. Romie, and V. D. Sanders
University of California

NACA

WASHINGTON

NACA ARR No. 5A08

NATIONAL ADVISORY COMMITTEE FOR AERONAUTICS

ADVANCE RESTRICTED REPORT

AN INVESTIGATION OF AIRCRAFT HEATERS

XX - MEASURED AND PREDICTED PERFORMANCE OF A FINNED-TYPE CAST-ALUMINUM CROSSFLOW EXHAUST GAS AND AIR HEAT EXCHANGER

By L. M. K. Boelter, A. G. Guibert, J. M. Rademacher, F. E. Romie, and V. D. Sanders

SUMMARY

Data on the thermal performance and the static pressure drop of a finned-type cast-aluminum exhaust gas and air heat exchanger are presented. One shroud, hereinafter designated as the UC-1 or full-crossflow shroud, was used for the tests on the heater.

The exhaust gas rates used in the tests ranged from 1740 to 5150 pounds per hour, and the ventilating air rates were varied from 1000 to 4500 pounds per hour. Static pressure drop measurements were made across the exhaust gas and ventilating air sides of the heater under isothermal and non-isothermal conditions.

The measured thermal outputs and static pressure drops are compared with predicted magnitudes. (See figs. 2, 3, 4, and 5.)

INTRODUCTION

The finned-type cast-aluminum exhaust gas and air heat exchanger was tested on the large test stand of the Mechanical Engineering Laboratories of the University of California. (See description of test stand in reference 1.) This heat exchanger is designed for use in the exhaust gas streams of aircraft engines for cabin heating systems and for wing- and tail-surface anti-icing systems.

The following data were obtained:

1. Weight rates of the exhaust gas and ventilating air through the respective sides of the heat exchanger

2. Temperatures of the exhaust gas and ventilating air at inlet and at outlet of the heater

3. Temperatures of the heater surfaces (exhaust gas side fins)

4. Static pressure drops across the exhaust gas and ventilating air sides of the heat exchanger for isothermal and non-isothermal conditions

This investigation, part of a research program conducted on aircraft heat exchangers at the University of California, was sponsored by and conducted with the financial assistance of the National Advisory Committee for Aeronautics.

SYMBOLS

A area of heat transfer; and cross-sectional area of a fin, ft^2

A_{cs} cross-sectional area of flow for either fluid, ft^2

A_h cross-sectional area of flow for either fluid, measured within the heater, ft^2

A_u area of heat transfer measured over unfinned surface, ft^2

A_1 cross-sectional area of flow for either fluid, taken at inlet pressure measuring station, ft^2

A_2 cross-sectional area of flow for either fluid, taken at outlet pressure measuring station, ft^2

c_p heat capacity of fluid at constant pressure, Btu/lb °F

D hydraulic diameter, ft

D_c base diameter of circumferential air-side fins, ft

f_c unit thermal convective conductance for either fluid (average with length), Btu/hr ft^2 °F

f_f unit thermal convective conductance of either fluid flowing over a fin (average with length), Btu/hr ft^2 °F

f_u unit thermal convective conductance of either fluid flowing over unfinned surfaces, using hydraulic diameter D as significant dimension in equation (6) (average with length), Btu/hr ft^2 °F

$(f_cA)_e$ "effective" thermal conductance of a finned surface, Btu/hr °F

$(f_cA)_u$ thermal conductance of fluid flowing over unfinned portion of finned surface, Btu/hr °F

g gravitational force per unit of mass, lb/(lb sec^2/ft)

G weight rate of fluid per unit of cross-sectional area, lb/hr ft^2

k thermal conductivity of fin material, Btu/hr ft^2(°F/ft)

K isothermal pressure drop factor, defined by the equation $\frac{\Delta P}{\gamma} = K \frac{u_m^2}{2g}$

l longitudinal length of a fin; and length of a duct measured from the entrance, ft

L length of a fin projecting into fluid stream, ft

m ratio of cross-sectional area of flow before expansion to that after expansion

n number of fins on either side of heater

P heat transfer perimeter of one fin on either side of heater, ft

q measured rate of enthalpy change of fluid, Btu/hr or kBtu/hr (kBtu designates kilo Btu, or 1000 Btu/hr)

s thickness of one fin, ft

T_{av} arithmetic average mixed-mean absolute temperature of either fluid $\frac{T_1 + T_2}{2}$, °R

T_{iso} mixed-mean absolute temperature of fluid for isothermal pressure drop tests, °R

T mixed-mean absolute temperature of fluid, °R

u_m mean velocity of fluid at minimum cross-sectional area of fluid passages, ft/sec

UA over-all thermal conductance, Btu/hr °F

W weight rate of fluid, lb/hr

γ weight density of fluid, lb/ft^3

ΔP static pressure drop, lb/ft^2

$\Delta P''$ over-all static pressure drop (heater plus ducts) on either side, inches H_2O

ΔP_{contr} isothermal static pressure drop due to a sudden contraction in flow passage on either side of heater, lb/ft^2

ΔP_{exp} isothermal static pressure drop due to a sudden expansion in flow passage on either side of heater, lb/ft^2

ΔP_{fric} isothermal static pressure drop due to friction alone, lb/ft^2

ΔP_{htr} isothermal static pressure drop across heater alone, lb/ft^2

ΔP_{iso} over-all isothermal static pressure drop along heater and ducts at temperature T_{iso}, lb/ft^2

Δt_{mx} mean temperature difference for crossflow as defined by equation (43) of reference 2, °F

ζ isothermal friction factor defined by the equation $\frac{\Delta P_{iso}}{\gamma} = \zeta \frac{l}{D} \frac{u_m^2}{2g}$

μ absolute viscosity of either fluid, lb sec/ft^2

τ mixed-mean temperature of fluid, $^\circ$F

Re Reynolds number ($GD/3600\mu g$)

Subscripts

a ventilating air side

c convective conductance f_c, circumferential fins D_c, and sudden contraction K_c

cs cross-sectional areas

e "effective" thermal conductance $(f_cA)_e$ and sudden expansion K_e

f fins or finned surfaces

g exhaust gas side

u unfinned surfaces

1 entrance

2 exit section

DESCRIPTION OF HEATER AND TESTING PROCEDURE

The finned-type cast-aluminum heat exchanger tested is a crossflow unit with longitudinal fins on the exhaust gas side and with circumferential fins on the ventilating air side. (See figs. 1, 6, and 7.)

The heater consists of a cast tube of aluminum with 30 fins cast on the interior (gas side) and with 68 circumferential fins machined on the exterior (ventilating air side). The internal fins are wedge-shape and taper in length near the ends of the heater, the length of the fins being 1.28 inches and the over-all depth 1 7/8 inches. The external (ventilating air side) circumferential fins are 1 3/16 inches long with parallel sides on a base which has a diameter of 6 inches. At each end of the heater on the

ventilating air side, the length of the outermost fins is only 19/32 inch. From this last fin to the twelfth fin inward, the length is increased regularly to the maximum of $1^{1}/_{16}$ inches. The surface of the walls of the internal fins is as cast – that is, very rough; whereas all other surfaces of the heater are machined – that is, relatively smooth. (See discussion of exhaust gas side pressure drop for consideration of one effect of this roughness.)

The air shroud used, designated as UC–1 in this report, is designed to give full–crossflow characteristics. Photographs of the heater are shown in figures 6 and 7.

Calibrated square–edge orifices were used for the measurement of the weight rates of exhaust gas and ventilating air.

The temperatures of the exhaust gas were measured with traversing shielded thermocouples. Unshielded traversing thermocouples were employed for measurement of the temperatures of the ventilating air.*

Temperatures of the heater surfaces were measured at two points on the exhaust gas side fins at the entrance to the heater.

Static pressure drop measurements were obtained across the ventilating air and exhaust gas sides of the heater. Two taps, 180° apart, were installed at each pressure–measuring station.

Heat transfer and static pressure drop data for the exchanger using this shroud are presented in tables I to III. Plots of these data as functions of the weight rates of the ventilating air and exhaust gas are presented in figures 2 to 5.

---

*Because this thermocouple was not shielded from radiation to the relatively cooler walls, a temperature slightly lower than the true air temperature was obtained. A calculation shows the error to be less than 1 percent of the temperature rise of the air as it passes through the heater.

METHOD OF ANALYSIS

Heat Transfer

The thermal output of the exchanger was determined from the enthalpy change of the ventilating air:

$$q_a = W_a \, c_{p_a} (\tau_{a_2} - \tau_{a_1}) \qquad (1)$$

in which c_{p_a} was evaluated at the arithmetic average ventilating air temperature. A plot of q_a against W_a at constant values of the exhaust gas rate W_g is presented in figure 2.

For the exhaust gas side of the heater

$$q_g = W_g \, c_{p_g} (\tau_{g_1} - \tau_{g_2}) \qquad (2)$$

where c_{p_g} is taken as that of air* at the average exhaust gas temperature. Ideally, for the case of a heat exchanger thermally insulated from its surroundings, q_g would equal q_a. Because experience has shown q_a to be the more reliable value, it is used in determining the over-all thermal conductance UA. The heat balance ratios q_g/q_a are given in table I.

---

*This approximation is permissible here because the fuel-air ratio of the exhaust gases used in these tests was extremely lean. In calculations of the performance of a heat exchanger when using exhaust gases, it is suggested that the heat capacity c_p of the mixture be computed, using the data for the heat capacity of the pure component as given in reference 7.

The over-all thermal conductance UA was evaluated from the expression

$$q_a = (UA)\Delta t_{mx} \tag{3}$$

where Δt_{mx} is the mean effective temperature difference for crossflow of fluids.* This term is shown graphically in figure 31a of reference 2 as a function of the terminal temperatures of the exhaust gas and ventilating air. The variation of UA with W_a, using W_g as the parameter, is shown in figure 3.

The thermal output of the heater for values of Δt_{mx} and weight rates other than those used here may be predicted by determining UA at the desired weight rates from figure 3 and using these magnitudes in equation (3).**

Predictions of the magnitude of the over-all thermal conductance UA were attempted. The expression

$$UA = \frac{1}{\left(\frac{1}{f_c A}\right)_{ea} + \left(\frac{1}{f_c A}\right)_{eg}} \tag{4}$$

was used. (See reference 2, equation (46)).

The effective thermal conductances for the two finned surfaces, $(f_c A)_{ea}$ and $(f_c A)_{eg}$, are determined from the equations

---

*Both fluids are postulated to be unmixed as each passes through the heat exchanger.

**This method is an approximation only, because the over-all thermal conductance UA is a function of the temperatures of the fluids $UA \propto f_c \propto T^{0.3}$, and this fact must be considered when the change in q_a for a fixed change in the mean effective temperature difference Δt_{mx} is desired. (See appendix A, reference 3, for a discussion of the approximation and of the complete correction.)

$$(f_c A)_{ea} = \pi D_c \; n \sqrt{2 f_f k s} \left(1 + \frac{L}{D_c}\right) \tanh \sqrt{\frac{2 f_f L^2}{k s}} + f_u A_u \qquad (5)$$

for the air side circumferential fins, and

$$(f_c A)_{eg} = n l \sqrt{2 f_f k s} \tanh \sqrt{\frac{2 f_f L^2}{k s}} + f_u A_u \qquad (6)$$

for the gas side fins (reference 2, equations (36) and (38))

where

n number of fins

f_f unit thermal convective conductance along fin

s thickness of fin

k thermal conductivity of fin material

L length of fin (projection of fin into fluid stream)

l longitudinal length of fin

D_c base diameter of circumferential air side fins

A_u unfinned heat transfer area

f_u unit thermal convective conductance on unfinned area

For both the air and gas sides of the heater, f_u was taken as being equal to the f_f along the fins on the corresponding side of the exchanger.

The unit thermal convective conductances f_f on the ventilating air and exhaust gas sides were evaluated from the following equation:

$$f_f = 5.4 \times 10^{-4} \, T_{av}^{0.3} \, \frac{G^{0.8}}{D^{0.2}} \left(1 + 1.1 \, \frac{D}{l}\right) \qquad (7)$$

In this equation D is the hydraulic diameter of the fluid passage, l the length of the passage in the direction of fluid flow, T_{av} the average absolute temperature of the

fluid, and G the weight rate per unit of free area normal to the fluid flow. All quantities are, of course, evaluated for conditions which exist on the air side or the gas side, depending on which side the f_f is calculated. The term $\left(1+1.1\frac{D}{l}\right)$ in equation (7) is a factor which corrects for the higher unit thermal conductance at the entrance of the duct. (See reference 4.) The use of this term has been justified approximately by experiments the results of which will be discussed in a report to be published in the near future. Inasmuch as this correction factor usually increases the unit thermal convective conductance by only a few percent (~ 3 to 7 percent), a slight change in the value of this term would not greatly affect the actual value of the unit thermal convective conductance.

Equation (7) is valid for straight smooth ducts, but inasmuch as roughness seems to have little effect upon the heat transfer in the turbulent regime (see reference 5, p. 198), and because so little is known about the variation of the unit conductance in ducts of complicated geometrical configuration, this equation is used as a good approximation.

Heat transfer by radiation from the fluids to the heater surfaces and also that from one surface to another are neglected in this analysis.

SAMPLE CALCULATION OF UA

(Based on Run 8, data from table I and fig. 3)

Computation of air side $(f_cA)_{ca}$

$$f_{fa} = 5.4 \times 10^{-4} \frac{T_{av}^{0.3} \; G_a^{0.8}}{D_a^{0.2}} \left(1+1.1\frac{D_a}{l}\right)$$

$$T_{av} = \frac{93 + 310}{2} + 460 = 662^{\circ} \text{ R}$$

$$D_a = \frac{4A_{cs}}{P} = \frac{4 \times 0.170}{27.8} = 0.0245 \text{ ft}$$

$$G_a = \frac{W}{A_{cs}} = \frac{1620}{0.170} = 9530 \text{ lb/hr ft}^2$$

$$\left(1 + 1.1\frac{D_a}{l}\right) = \left(1 + 1.1 \times \frac{0.0245}{0.925}\right) = 1.029$$

$$f_{f_a} = 5.4 \times 10^{-4} \frac{662^{0.3} \times 9530^{0.8} \times 1.029}{0.0245^{0.2}} = 12.5 \text{ Btu/hr } ^\circ\text{F ft}^2$$

Effective thermal conductance

$$(f_cA)_{ea} = \pi D_c\, n \sqrt{2f_f ks}\left(1 + \frac{L}{D_c}\right) \tanh \sqrt{\frac{2f_f L^2}{ks}} + f_u A_u \qquad (5)$$

$D_c = 0.5$ ft

$n = 62$ fins (equivalent number of fins of length 0.0885 ft)

$k = 125$ Btu/hr ft^2 ($^\circ$F/ft)

$s = 0.00584$ ft

$L = 0.0885$ ft

$f_f = f_u$

$(f_uA_u)_a = 12.5 \times 1.20 = 15.0$ Btu/hr $^\circ$F

$$(f_cA)_{ea} = \pi \times 0.5 \times 62 \sqrt{2 \times 12.5 \times 125 \times 0.00584}\left(1 + \frac{0.0885}{0.5}\right) \tanh \sqrt{\frac{2 \times 12.5 \times 0.0885^2}{125 \times 0.00584}} + 15.0$$

$(f_cA)_{ea} = 233 + 15 = 248$ Btu/hr $^\circ$F

Computation of the thermal conductance of the gas side

$$f_{f_g} = 5.4 \times 10^{-4} \frac{T_{av}^{0.3}\, G_g^{0.8}}{D_g^{0.2}}\left(1 + 1.1\frac{D_g}{l}\right)$$

$$T_{av} = \frac{964 + 871}{2} + 460 = 1378^\circ \text{ R}$$

$$D_g = \frac{4A_{cs}}{P} = \frac{4 \times 0.111}{7.50} = 0.0592 \text{ ft}$$

$$G_g = \frac{W}{A_{cs}} = \frac{3240}{0.111} = 29{,}200 \text{ lb/hr ft}^2$$

$$\left(1+1.1\,\frac{D_g}{l}\right) = \left(1 + \frac{1.1 \quad 0.592}{1.17}\right) = 1.056$$

$$f_{f_g} = 5.4 \times 10^{-4} \times \frac{1378^{0.3} \times 29200^{0.8} \times 1.056}{0.0592^{0.2}} = 32.5 \text{ Btu/hr ft}^2\,^{\circ}\text{F}$$

Effective thermal conductance

$$(f_cA)_{eg} = n\,L\,\sqrt{2f_f k s}\,\tan\sqrt{\frac{2f_f L^2}{ks}} + (f_uA_u)_g \qquad (6)$$

$h = 30$

$L = 1.085$ ft

$s = 0.0156$ ft

$k = 145$ Btu/hr ft^2 ($^{\circ}$F/ft)

$f_f = 32.5$ Btu/hr ft^2 $^{\circ}$F

$(f_uA_u)_g = 32.5 \times 0.932 = 30.0$

$$(f_cA)_{eg} = 30 \times 1.085\,\sqrt{2 \times 0.0156 \times 145 \times 32.5}\,\tanh\sqrt{\frac{2 \times 32.5 \times 0.107^2}{145 \times 0.0156}} + 30.0$$

$$= 204 + 30 = 234 \text{ Btu/hr }^{\circ}\text{F}$$

Computation of UA

$$\frac{1}{UA} = \frac{1}{(f_cA)_{ea}} + \frac{1}{(f_cA)_{eg}} = \frac{1}{248} + \frac{1}{234} = 0.00403 + 0.00427 = 0.00830$$

$UA = 121$ Btu/hr $^{\circ}$F

The experimentally obtained value of UA was 120 Btu/hr $^{\circ}$F.

PRESSURE DROP

Isothermal static pressure drop across the gas side of the heater was postulated to consist of four components: pressure drop due to converging and diverging ducts leading to and from the heater, contraction loss caused by fins as air enters the heater, the friction pressure loss within the finned portion of the heater, and the expansion loss due to the gas flow diverging upon leaving the finned portion of the heater.

The loss due to the converging and diverging ducts was determined experimentally by removing the heater and fitting the two sections together. It is doubtful whether the pressure drop so determined would agree with results obtained by measuring each section separately, but the difference, for the present purpose, is probably slight.

The contraction loss on entering the finned section of the heater was obtained from the equation

$$\frac{\Delta P_{contr}}{\gamma} = K_c \frac{u_m^2}{2g} \quad (K_c = 0.11) \tag{8}$$

where u_m is the mean velocity in the finned section of the heater and K_c is a "head loss" coefficient for sudden contraction obtained from reference 6, page 211.

Frictional pressure loss was calculated using the formula

$$\frac{\Delta P_{fric}}{\gamma} = \zeta \frac{l}{D} \frac{u_m^2}{2g} \tag{9}$$

where u_m is the mean velocity in the finned section and ζ is the friction factor for very rough pipe $\zeta \cong 0.050$. (See discussion of pressure drop.)

The expansion loss on leaving the fins was calculated from

$$\frac{\Delta P_{exp}}{\gamma} = K_e \frac{u_m^2}{2g} \quad (K_e = 0,096) \tag{10}$$

where u_m is again the mean velocity in the finned section and $K_e = (1-m)^2$, m being the ratio of the cross-sectional

area before expansion to that after expansion, K_e is a head loss coefficient for sudden expansion. (See reference 6, p. 211.) The over-all static pressure drop across the exhaust gas side of the heater was then the summation of these terms:

$$\frac{\Delta P_{htr}}{\gamma} = \frac{\Delta P_{contr}}{\gamma} + \frac{\Delta P_{fric}}{\gamma} + \frac{\Delta P_{exp}}{\gamma} \qquad (11)$$

Results of the measurements and calculations on exhaust gas isothermal pressure drop are given in table II and figure 5. They indicate a difference of only 7 percent between measured and predicted values of the isothermal static pressure drop.

The isothermal static pressure drop across the air side of the heater was predicted, but the calculations give pressure drops which are about 15 percent above the observed values mainly because the complicated flow path of the ventilating air could not be accurately analyzed. The pressure drop across the air side of the heater was calculated by means of the equations:

(a) Contraction loss as the ventilating air leaves the ducts and enters the heater section

$$\frac{\Delta P_{contr}}{\gamma} = K_c \frac{u_m^2}{2g} \qquad (K_c = 0.31) \qquad (8)$$

where K_c is the head loss coefficient for sudden contraction (approximation)

(b) Frictional pressure drop

$$\frac{\Delta P_{fric}}{\gamma} = \zeta \frac{l}{D} \frac{u_m^2}{2g} \qquad (9)$$

where ζ is taken as the friction factor for commercial pipe

(c) Expansion loss as the ventilating air leaves the heater section and enters the outlet duct

$$\frac{\Delta P_{exp}}{\gamma} = K_e \frac{u_m^2}{2g} \qquad (K_e = 0.49) \qquad (10)$$

where K_e is the head loss coefficient for sudden expansion, equal to $(1-m)^2$ where m is the ratio of the cross-sectional area before expansion to that after expansion.

The sum of these heater losses was then compared with the observed pressure drop (due to the heater alone). Because the measured isothermal pressure drop consisted of the pressure drop across the heater plus that across the inlet and outlet shroud ducts, it was necessary, in order to compare the calculated and the "observed" pressure drops, to determine experimentally the additional pressure drop due to these ducts. This static pressure drop which was measured for the ducts alone, was subtracted from the measured isothermal static pressure drop across the heater-shroud combination, and the result termed the observed pressure drop due to the heater alone ΔP_{htr}. Results of these calculations are presented in table II. Figure 4 shows the measured isothermal pressure drop and the predicted isothermal pressure drop (obtained by adding the predicted static pressure drop due to the heater alone ΔP_{htr} and the measured duct-shroud loss) plotted as a function of the air rate.

Non-isothermal pressure drop.- The non-isothermal static pressure drop for either side of the heat exchanger was predicted from the measured isothermal static pressure drop for that side using the equation (see reference 2, equation (54))

$$\Delta P_{non\text{-}iso} = \Delta P_{iso}\left(\frac{T_{av}}{T_{iso}}\right)^{1.13} + \left(\frac{W}{3600}\right)^2 \frac{1}{2g\,\gamma_1}\frac{1}{A_h^2}\left[\left(\frac{A_h^2}{A_2^2}+1\right)\frac{T_2}{T_1} - \left(\frac{A_h^2}{A_1^2}+1\right)\right] \quad (12)$$

in which ΔP_{iso} is the total measured isothermal static pressure drop at temperature T_{iso}; T_1 and T_2 are the mixed-mean absolute temperatures of the fluid at the inlet and outlet of the heater, respectively; T_{av} is the arithmetic average of T_1 and T_2; W is the weight rate of fluid; γ_1 is the weight density of the fluid, evaluated at temperature T_1; A_1 and A_2 are the cross-sectional duct areas at the upstream and downstream pressure taps, respectively; and A_h is the cross-sectional area of flow in the heater.

A comparison of measured and predicted non-isothermal pressure drops across each side of the heater is presented in table III and is shown graphically in figures 4 and 5.

DISCUSSION

The results of the tests on the cast-aluminum finned-type heat exchanger are shown graphically in figures 2 to 5. The graphs are based on the data presented in tables I to III.

Heat Transfer

The predictions of the over-all thermal conductance for this cast-aluminum heater, using the full-crossflow shroud, are on the average within 4 percent of the experimental values. The calculations indicate that the controlling resistance to heat transfer is on the exhaust gas side at the two lower exhaust gas rates (~1740 and 3240 lb/hr). This would mean that an increase of the cross-sectional area of flow on the gas side of the heater for the purpose of reducing the high pressure drop which occurs across this side should be undertaken with caution because such a change of the gas side might appreciably reduce the heat transfer performance for these gas rates. It must also be kept in mind that for a fixed air side resistance, a higher thermal resistance on the exhaust gas side produces a lowered metal surface temperature.

Investigations (see reference 5, p. 198) have shown that roughness has little effect upon the heat transfer from fluids and therefore the roughness of the surface of the gas side fins was neglected in this analysis. The effect of curvature upon the heat transfer from the heater surfaces to the ventilating air was omitted because there appears to be no general correlation among the experimental data in the literature.

Isothermal Pressure Drop

The predicted isothermal static pressure drop across the air side of the heater was based upon the frictional pressure drop along the curved flow-path and on the contraction and expansion losses which occur as the ventilating air enters and leaves this flow path over the heater. Although the effect of curvature was neglected, the predicted values of the isothermal static pressure drop were higher than the measured values. The explanation of this deviation lies, perhaps, in

the fact that the contraction and expansion were considered as occurring suddenly, which is, of course, only a first approximation. In conformity with previous reports, the friction factor used in calculating the air side frictional static pressure drop was taken as that for smooth commercial pipe. Justification of the choice of this friction factor lies in the smooth machined surface of the circumferential fins.

The isothermal static pressure drop across the exhaust gas side of this heater was attempted, using the same choice of a friction factor (smooth commercial pipe). When this procedure was used, however, the difference between predicted and observed values of the pressure drop indicated that the rough, as cast, surfaces of the exhaust gas side fins must be considered in evaluating the friction factor for use in equation (9). Trial calculations showed that use of a friction factor of the magnitude $\zeta = 0.050$ would predict pressure drops which are only slightly less than those which were observed. If Nikuradse's results are used for the variation of the friction factor with roughness at any fixed value of the Reynolds number (see reference 6, p. 107) it is possible to predict a friction factor of the desired magnitude $\zeta \cong 0.050$. Because this friction factor is so great (about the magnitude of that of concrete pipe), it can be said, from a consideration of the effect upon the frictional pressure drop, that it is desirable to machine these rough surfaces, if possible. Predicted isothermal pressure drops for the gas side, using this friction factor, are given in table II and are plotted as a function of the exhaust gas rate in figure 5.

A head loss coefficient to take into account both friction and other losses within the heater was computed on the basis of the equation:

$$\frac{\Delta P_{htr}}{\gamma} = K \frac{u_m^2}{2g} \qquad (13)$$

The values of K obtained for the exhaust gas side of this heat exchanger were of the order of 1.3; whereas those for the ventilating air side were of the order of 2.0. These values of the head loss coefficient permit a rough estimate of the pressure drop in similar heater sections. (See previous reports of this series for values of the head loss coefficients for other heater systems.)

Non-isothermal Pressure Drop

Predictions of the non-isothermal static pressure drops

from the measured isothermal pressure drops were attempted for both sides of the heater. On the air side, the predictions were within 3 percent of the observed values, though the slope of the predicted curves was greater. On the gas side, the predictions were about 30 percent higher than the observed values, but the slopes of the curves were essentially the same. These predictions are shown in the plots of pressure drop against weight rate of fluid. (See figs. 4 and 5.)

Heater Surface Temperatures

Temperatures of the heater surface were taken at two points on the exhaust gas side fins. Two thermocouples were inserted at the tips of two of the fins at a point near the inlet end of the heater. The sole difference in the location of these two thermocouples was that one was inserted in a fin of slightly thicker cross section than the other fin. The junction of each thermocouple was located just below the surface of the fin. The maximum surface temperatures recorded during the series of runs (inlet temperature of exhaust gas $\cong$ 1000° F) were 745° F for the thicker fin and 795° F for the other.

The melting point of aluminum is approximately 1200° F, and, in view of the heater surface temperature ($\sim$ 800° F) recorded with an inlet gas temperature of 1000° F, it would not be entirely safe to use this heater in exhaust gas streams where the inlet gas temperature is 1400° F or more. Even at the temperatures used in these tests, there were some slight indications of melting at the surfaces where the hot exhaust gases impinged upon the fins.

CONCLUSIONS

1. The thermal performance of a crossflow unit with circumferential fins on the air side and longitudinal fins on the gas side was predicted within 4 percent.

2. The isothermal static pressure drop across such a unit was predicted to within 15 percent on the air side and within 7 percent on the exhaust gas side.

3. By use of the isothermal static pressure drop, the non-isothermal static pressure drop across the ventilating air side was predicted within approximately 3 percent, and

that across the exhaust gas side was predicted within approximately 30 percent.

4. The isothermal friction factor on the exhaust gas side was exceptionally high owing to the roughness of the as-cast surfaces of the fin walls.

University of California,
Berkeley, Calif., July 1944.

REFERENCES

1. Boelter, L. M. K., Miller, M. A., Sharp, W. H., Morrin, E. H., Iversen, H. W., and Mason, W. E.: An Investigation of Aircraft Heaters. IX - Measured and Predicted Performance of Two Exhaust Gas-Air Heat Exchangers and an Apparatus for Evaluating Exhaust Gas-Air Heat Exchangers. NACA ARR, March 1943.

2. Boelter, L. M. K., Martinelli, R. C., Romie, F. E., and Morrin, E. H.: An Investigation of Aircraft Heaters. XVIII - A Design Manual for Exhaust Gas and Air Heat Exchangers. NACA ARR No. 5A06, 1945.

3. Boelter, L. M. K., Guibert, A. G., Rademacher, J. M., and Sloggy, L. J. B.: An Investigation of Aircraft Heaters. XIX - Performance of Two Finned-Type Crossflow Exhaust Gas and Air Heat Exchangers. NACA ARR No. 4H21, 1944.

4. Boelter, L. M. K., Dennison, H. G., Guibert, A. G., and Morrin, E. H.: An Investigation of Aircraft Heaters. X - Measured and Predicted Performance of a Fluted-Type Exhaust Gas and Air Heat Exchanger. NACA ARR, March. 1943.

5. McAdams, W. H.: Heat Transmission, McGraw-Hill Book Co., Inc., New York, N. Y., 1942, p. 198.

6. O'Brien, M. P., and Hickox, G. H.: Applied Fluid Mechanics. McGraw-Hill Book Co., Inc., New York, N. Y., 1937, pp. 107, 211-213.

7. Tribus, Myron, and Boelter, L. M. K.: An Investigation of Aircraft Heaters. II - Properties of Gases. NACA ARR, Oct. 1942.

TABLE-I - EXPERIMENTAL RESULTS ON FINNED-TYPE HEATER

A-4 CAST ALUMINUM HEATER — U C - I SHROUD

	AIR SIDE						EXHAUST GAS SIDE							HEATER TEMPS.			OVERALL PERFORM.	
Run	τ_{a_1}	τ_{a_2}	$\Delta\tau_a$	W_a	$\Delta P_a''$	q_a	τ_{g_1}	τ_{g_2}	$\Delta\tau_g$	W_g	$\Delta P_g''$	q_g	q_g/q_a	Gas Side Fin Temp			Δt_{m_x}	UA
No.	°F	°F	°F	Lb/hr	Inches H_2O	KBtu./hr.	°F	°F	°F	Lb/hr	Inches H_2O	KBtu./hr		°F	°F		°F	Btu./hr °F
3	88	227	139	4520	6.10	152	960	858	102	5140	19.7	137	0.90	700	595		750	203
2	86	278	192	3180	3.63	148	1044	947	97	5170	21.9	131	0.88	—	—		805	183
1	86	312	226	2280	2.12	125	1036	943	93	5150	22.1	125	1.00	795	740		790	158
6	95	252	157	2140	1.66	81.3	1006	875	131	1750	2.39	59.8	0.73	645	590		760	107
5	95	286	191	1590	1.04	73.4	998	879	119	1740	2.40	52.2	0.71	680	625		750	98
4	96	323	227	1020	0.48	56.1	1011	884	127	1740	2.38	57.7	1.03	730	695		740	75.7
7	94	275	181	2150	1.76	94.1	981	863	118	3260	7.84	100	1.07	705	645		740	127
8	93	310	217	1620	1.10	85.2	964	871	93	3240	7.89	78.7	0.92	735	685		710	120
9	93	359	266	1070	0.60	68.8	964	892	72	3230	7.96	60.6	0.88	775	745		700	98.3

TABLE II.- ISOTHERMAL STATIC PRESSURE DROP

Cast-Aluminum Heater Using Full-Crossflow Air Shroud

Run	W (lb/hr)	G (lb/hr ft²)	$\Delta P''_{iso}$ (meas.) (in. H_2O)	= $\Delta P''_{duct}$ (meas.) (in. H_2O)	+ $\Delta P''_{htr}$ (in. H_2O)	$\Delta P''_{htr}$ (pred.) (in. H_2O)	Re	K[a]	f
Exhaust Gas Side									
18	8000	72,100	23.0	1.70	21.3	17.7	92,400	1.29	0.045
16	4700	42,400	7.8	.60	7.20	6.62	54,400	1.26	.046
7	2900	26,200	3.10	.23	2.87	2.67	33,600	1.32	.049
5	1690	15,200	1.07	.08	.99	.99	19,500	1.35	.055
Ventilating Air Side									
10	1000	5,850	0.29	0.02	0.27	0.27	3,110	2.40	0.043
14	2680	15,700	1.78	.25	1.53	1.78	8,330	1.93	.038
20	5000	29,200	5.44	.90	4.54	5.83	15,500	1.65	.034

[a] K based on equation (13)

$$\frac{\Delta P_{htr}}{\gamma} = K \frac{u_m^2}{2g} \qquad (13)$$

where $\Delta P_{htr} = \Delta P''_{htr} \times 5.19$, lb/ft²

Note.- In figures 4 and 5, the curves labeled as "predicted isothermal pressure drop" are obtained by plotting the sum of the values $\Delta P''_{duct}$ (meas.) and $\Delta P''_{htr}$ (pred.) (columns 5 and 7 in this table).

TABLE III.- NON-ISOTHERMAL STATIC PRESSURE DROP DATA

Cast-Aluminum Heater Using Full-Crossflow Air Shroud

Run	W (lb/hr)	G (lb/hr ft^2)	T_1 ($^\circ$R)	T_2 ($^\circ$R)	T_{av} ($^\circ$R)	$\Delta P''_{iso}$ (in. H_2O)	$\Delta P''_{non-iso}$ [a] (pred.) (in. H_2O)	$\Delta P''_{non-iso}$ (meas.) (in. H_2O)
Exhaust Gas Side								
3	5140	46,300	1420	1318	1369	9.50	25.2	19.6
4	1740	15,700	1471	1344	1407	1.12	3.05	2.38
8	3240	29,200	1424	1331	1377	3.84	10.3	7.89
Ventilating Air Side								
2	3180	18,600	546	738	642	2.35	3.62	3.60
8	1620	9,470	553	770	661	.71	1.11	1.10
4	1020	5,960	556	783	669	.30	.47	.46

[a] Predictions based on equation (12)

$$\Delta P_{non-iso} = \Delta P_{iso} \left(\frac{T_{av}}{T_{iso}}\right)^{1.13} + \left(\frac{W}{3600}\right)^2 \frac{1}{2\nu_1 g A_h^2} \left[\left(\frac{A_h^2}{A_2^2} + 1\right)\frac{T_2}{T_1} - \left(\frac{A_h^2}{A_1^2} + 1\right)\right] \qquad (12)$$

$\Delta P = \Delta P'' \times 5.19$, lb/ft^2

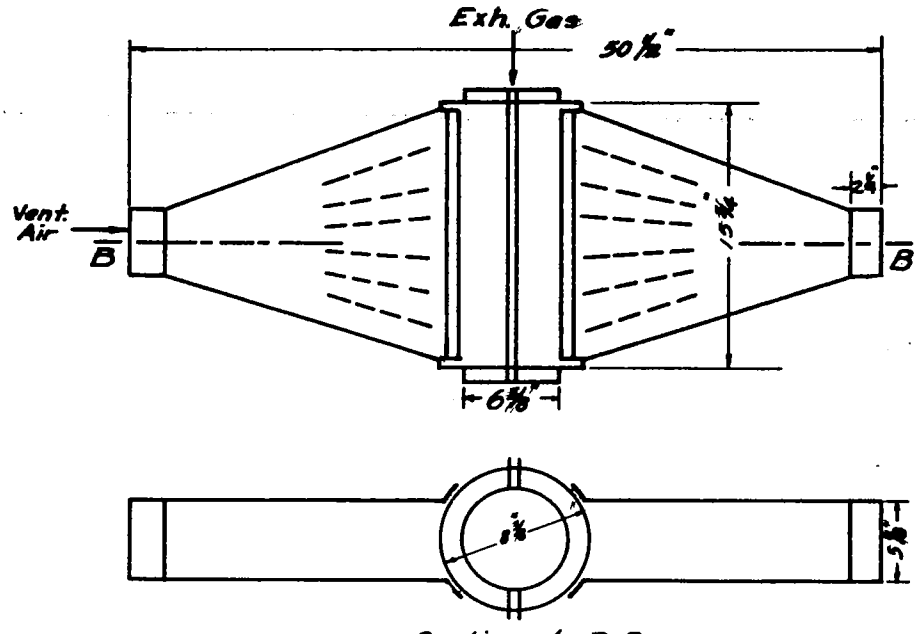

Section at B-B
UC-1 Air Shroud

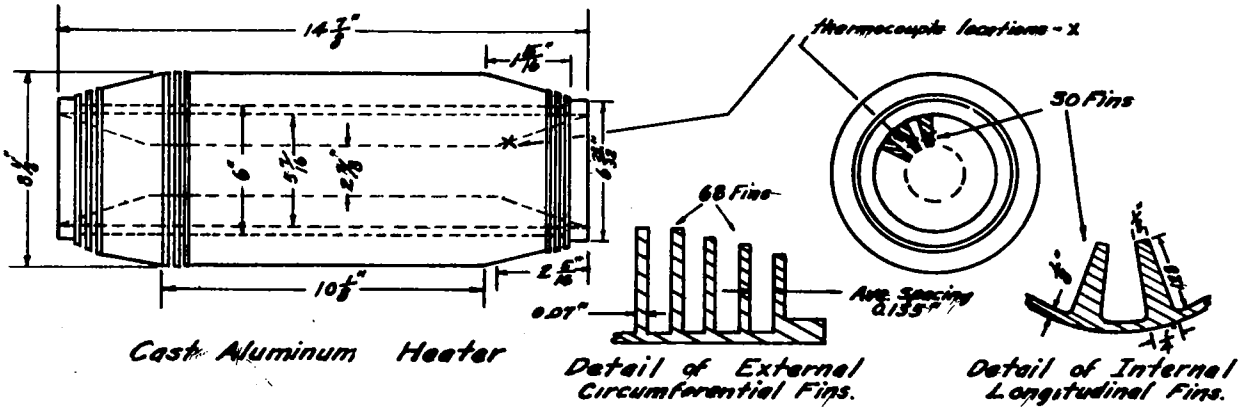

Cast Aluminum Heater

Detail of External Circumferential Fins.

Detail of Internal Longitudinal Fins.

CAST ALUMINUM HEATER

Weight	Air Side	Gas Side
31.0 Lbs.		
Cross-sectional Area ft²	0.170	0.111
Total Wetted Perimeter Ft.	27.8	7.50
Hydraulic Diameter ft.	0.0245	0.0592

Fig. 1- Schematic Diagram of Cast Aluminum Finned Type Heat Exchanger

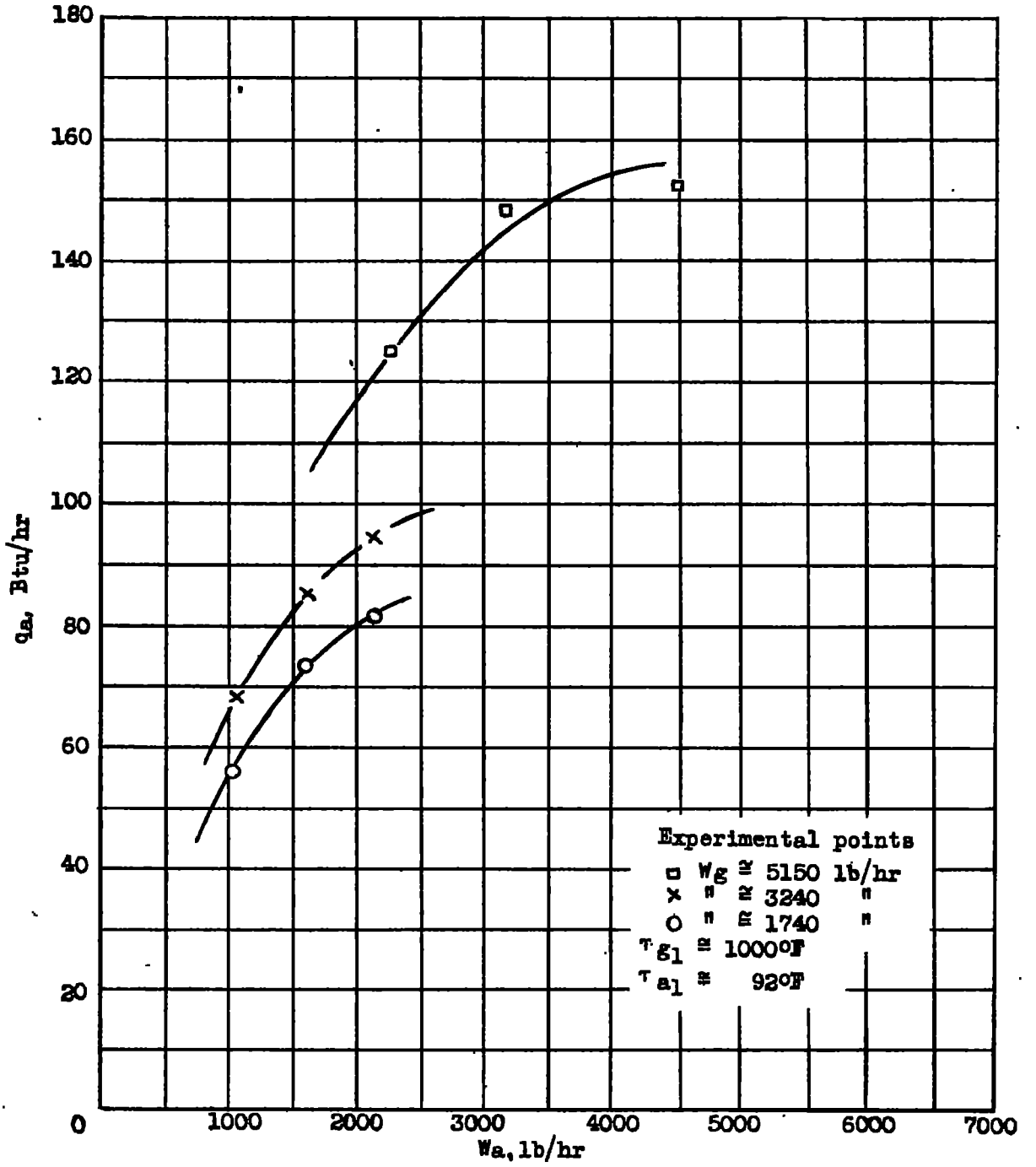

Figure 2.- Thermal output of an aluminum finned-type heater as a function of ventilating air rate.

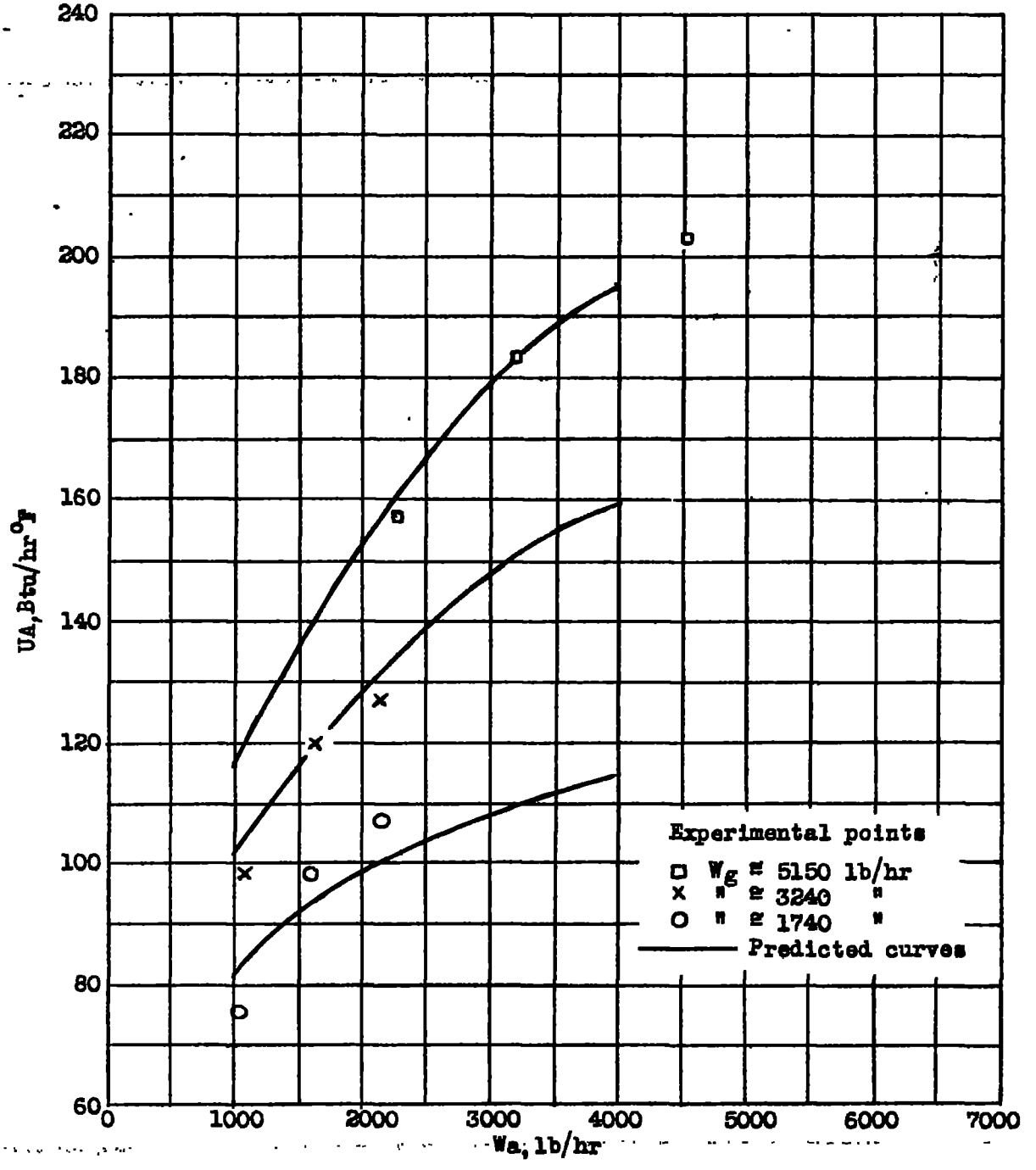

Figure 3.- Overall thermal conductance of an aluminum finned-type heater as a function of ventilating air rate.

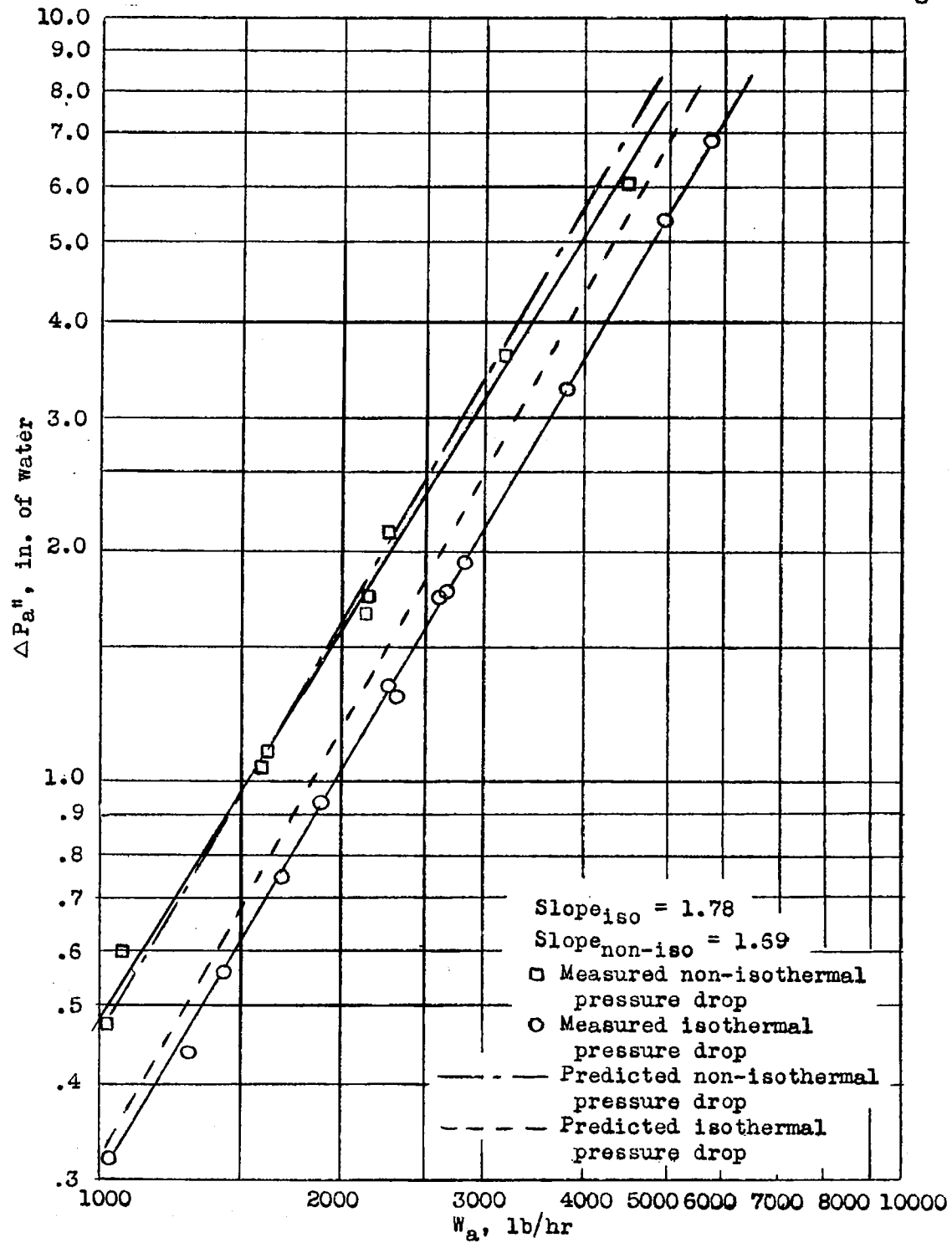

Figure 4.- Static pressure drop on air side of aluminum finned-type heater as a function of ventilating air rate.

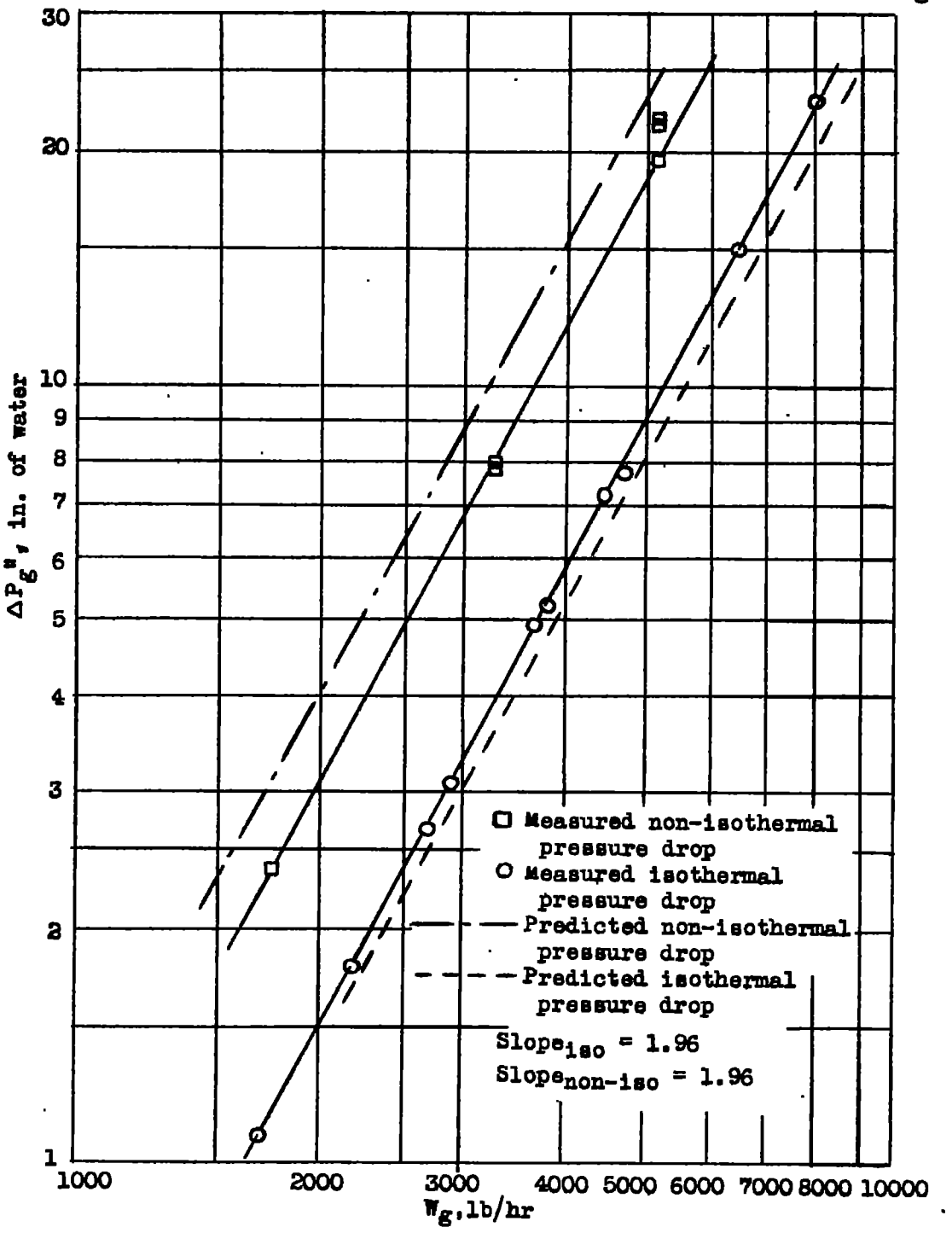

Figure 5.- Static pressure drop on the gas side of an aluminum finned-type heater as a function of ventilating air rate.

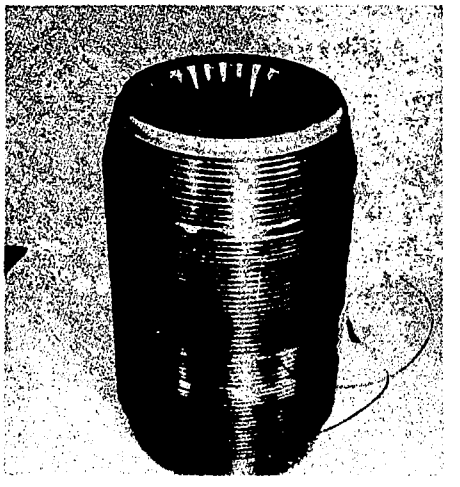

Figure 6.- Photograph of finned-type cast-aluminum crossflow heat exchanger.

Figure 7.- Photograph of finned-type cast-aluminum crossflow heat exchanger.